DOI: 10.1021/ma101780h

Macromolecules
ARTICLE

Functionalization of Multi-Walled Carbon Nanotubes by Stereoselective Nucleophilic Substitution on PVC

Horacio J. Salavagione,*,† Gerardo Martínez,† and Carmen Ballesteros‡

†*Instituto de Ciencia y Tecnología de Polímeros, CSIC, Juan de la Cierva 3, 28006 Madrid, Spain, and*
‡*Departamento de Física, Universidad Carlos III de Madrid, Avenida Universidad 30, 28911 Leganés, Spain*

Received August 4, 2010; Revised Manuscript Received October 8, 2010

ABSTRACT: In this article, multiwalled carbon nanotubes (MWNT) soluble in common organic solvents are prepared. The solubility is conferred to the MWNTs by covalent attaching of appropriately modified poly(vinyl chloride)(PVC). The nucleophilic substitution of PVC with potassium 4-hydroxythiophenolate is carefully studied. It proceeds through a stereoselective mechanism. The subsequent esterification reaction of the hydroxyl pendant groups in the modified PVC (mPVC) with carboxylic acids created in MWNT is reported. The intermediates and final products are characterized by FTIR, ^{1}H and ^{13}C NMR, and Raman spectroscopy. The thermal stability as well as the molecular dynamics of the MWNT-modified PVC (MWNT-mPVC) are studied. The potential applications of the PVC-functionalized carbon nanotubes and the demonstrated functionalization strategy are discussed.

Introduction

Carbon nanotubes (CNTs) have attracted much attention among scientists in various disciplines since their discovery in 1991.[1] Both single-walled carbon nanotubes (SWNTs) and multi-walled carbon nanotubes (MWNTs) possess tubular nanostructures with unique properties and are promising materials for engineering applications[2] such as polymer composites, electronic devices, field emission displays, hydrogen storage, etc. However, manipulation and processing of CNTs have been limited by their insolubility in most common solvents. Many approaches have been employed to anchored functional groups on the surface of CNTs to solubilize these useful materials and facilitate their studies.[3,4] Several reports described the functionalization of the carboxylic acid groups located at the ends and defect sites by using thionyl chloride and subsequent reactions of the resulting acyl chloride.[5−7] Recently, dispersions of raw CNTs have been subjected to ozonolysis followed by treatment with various reagents, in independent runs, to generate a higher proportion of carboxylic acid/ester, ketone/aldehyde, and alcohol groups respectively, on nanotube surface.[8,9] Sidewall functionalization has also been achieved in a few cases using organic reagents.[10,11] Furthermore, the addition of aromatic amines to SWNTs has also been attempted.[12] Dissolved lithium metal in liquid ammonia is used to hydrogenate SWNT.[13] Finally, free radicals generated by decomposition of organic peroxide in the presence of alkyl iodides have been used to modify small-diameter SWNTs.[14,15]

Among the various functionalization strategies, the grafting of polymer instead of low-molecular-weight compounds on CNTs is a powerful strategy for the preparation of tubes with little damage in structure and high solubility.[16] In that sense, "grafting from" and "grafting to" approaches have been explored.[17−19] The former allows high bonding density, with amounts of grafting polymers as high as 70 wt %. However, control over the molecular weight and architecture of grafting polymers might be difficult. In contrast, the latter is a modular approach in which polymers can be prepared prior to the grafting step, and thus their molecular size and architecture can be well controlled.[20] Various polymers have been successfully grafted onto the nanotube surface via the "grafting to" strategy involving radical coupling,[18] nitrene addition,[16,21] click coupling,[22] nucleophilic reaction of polymeric carbanions,[23] and reactions with carboxyl groups on oxidized nanotubes.[24]

The solubilization of CNTs, especially those from the polymer functionalization, is considered as an effective way to achieve a homogeneous dispersion of CNTs in polymer matrices for high-quality nanocomposites. For example, Sun et al. solubilized CNTs through the covalent attachment of different polymers (polystyrene copolymer,[24a] poly(vinyl alcohol),[24c] and polyimide derivatives[24d]) and then dispersed the polymers-functionalized CNTs into new polymer matrices for the fabrication of nanocomposites. MWNTs, covalently functionalized with chlorinated polypropylene, have been used as the filler material in polymer/nanotube composites using polystyrene and poly(vinyl chloride) (PVC) as the polymer matrix.[23] Poly(*n*-butyl methacrylate) (PBMA) has been grafted onto MWNTs using atom transfer radical polymerization (ATRP) and the enhancement of the mechanical performance of PVC using PBMA-*g*-MWNTs as filler has been studied. The miscibility between PVC and PBMA enabled the homogeneous dispersion of nanotubes in the PVC matrix and improved the efficiency of load transfer from the matrix to the nanotubes.[25]

On the other hand, nucleophilic substitution of chlorine in PVC by a series of functional groups has been viewed as an appropriate method to improve properties, such as the thermal stability, by replacing of labile chlorines, and the mechanical properties by grafting functions that are capable of provoking cross-linking or graft copolymers.[26−28] Besides, the prominent role of the tacticity-governed microstructure on the chemical reactivity has been recently reported.[29,30] Finally, the preparation of nanocomposites of PVC with carbon nanotubes has been reported.[31−33] However, to the best of our knowledge, covalent functionalization of CNTs with PVC has never been approached.

In this work, we report an efficient "grafting to" method to prepare polymer functionalized MWNTs. The method lies in the introduction of pendant hydroxyl groups the PVC for subsequent

*Corresponding author. Telephone: +34-915622900x2. Fax: +34-915644853 08. E-mail: horacio@ictp.csic.es.

 Published on Web 11/03/2010

Table 1. Triad Probability and Glass-Transition Temperature of PVC and Their Substituted Samples

sample	degree of substitution (mol %)	P_{rr}[a]	$P_{mr} + P_{rm}$[a]	P_{mm}[a]	ρ[b]	T_g (°C)
PVC		0.292	0.498	0.210	0.997	78.8
mPVC1	4.6	0.337	0.455	0.162	0.966	87.4
mPVC2	13.2	0.384	0.380	0.103	0.885	98.3
mPVC3	15.2	0.395	0.360	0.093	0.872	101

[a] Probability of syndio (P_{rr}), hetero ($P_{mr} + P_{rm}$), and isotactic (P_{mm}) triads. [b] Persistence ratio.[36]

esterification reactions with carboxylic groups on the MWNTs surface. The resulting PVC-functionalized MWNTs were found to be soluble in the same solvents as the parent PVC. A significant advantage with this approach is that the functionalized nanotube samples have been prepared from a stereoselective nucleophilic substitution reaction what allow us to merge the control of the reaction and the good properties of nanotubes and, consequently, to enhance the properties of the PVC.

Experimental Section

Materials. A PVC sample was prepared at 90 °C in a bulk polymerization process (20% conversion) with 2, 2′-azobisisobutyronitrile (AIBN) as initiator. The degree of isotacticity was determined by FTIR and ^{13}C NMR. Tetrahydrofuran (THF, Ferosa), cyclohexanone (CH, Aldrich), *N*-methyl-2-pyrrolidone (NMP, Aldrich), and hexamethylphosphoric triamine (HMPT, Aldrich) were purified by fractional distillation under nitrogen. *N*,*N*-Dicyclohexylcarbodiimide (DCC), 4-(dimethylamino) pyridine (DMAP, 99%), and 4-hydroxythiophenol of technical grade (HT, 90%) were purchased from Aldrich and used as received. Equimolecular amounts of HT and potassium carbonate (K_2CO_3) were used to form 4-hydroxythiophenolate anion "in situ" in CH. Deuterated solvents for NMR measurements were purchased from Aldrich. MWNTs (length: 1−10 μm, average outside diameter of 13 nm, no amorphous carbon, bulk density: 150 g/L, and purity: >95%) prepared via chemical vapor deposition (CVD) were a generous gift by Bayer (Baytubes C 150P).

Substitution Reaction of PVC with Potassium 4-Hydroxythiophenolate (KHT). A 1 g (16.0 mmol, based on monomeric unit) sample of PVC was dissolved in 100 mL of CH, and 2.2 g (15.9 mmol) of K_2CO_3 and 2.0 g (15.9 mmol) of HT were added to the polymer solution. The mixture was stirred and heated at 40 °C under inert atmosphere. At appropriate reaction times, samples were precipitated in methanol−water mixtures, purified in THF/methanol−water as solvent/precipitant system and dried under vacuum at 40 °C. The degree of substitution of PVC was calculated by ^{1}H NMR spectroscopy (Table 1). Briefly, the extent of modificacion was estimated by comparing the integrated intesities of the aromatic protons signal due to the modifying group (δ = 7.5−6.9 ppm) against that corresponding to methinic protons in the pure PVC (δ = 4.9−4.5 ppm).

Ozonolysis of Carbon Nanotubes. MWNTs were ozonized by using a commercial Fisher model 500 ozonolysis apparatus at room temperature. In this instrument, the flow of O_2 to the arc discharge is kept below 2 psi. Ozone was formed in a 180 W discharge with the pressure adjusted to maintain a constant flow of a ~ 10% O_3 in oxygen mixture to the sample at a pressure lower than 2.5 psi. Typically, 150 mg samples were first dispersed in 60 mL of NMP by extensive sonication. The reaction mixture was stirred vigorously during ozonolysis, which was carried out for 4 h to create the expected ozonide intermediate. The reaction mixture was then flushed with O_2 at the end of ozonolysis to eliminate remaining O_3. The expected primary ozonides generated were cleaved by addition of ~10 mL of 50% H_2O_2 in aqueous solution at 70 °C for 4 h. The H_2O_2-cleaved tubes were then filtered over a 0.2 μm polycarbonate membrane and washed with a large excess of 50% HCl solution, followed by copious amounts of deionized water. The filtered MWNT were dried at 80 °C overnight.

Nanotube Functionalization. The ozonized MWNTs were functionalized with the modified-PVC (mPVC) in cabodiimide-activated esterification reactions.[7] In a typical experiment, DCC (2.12 g, 10.2 mmol) and DMAP (0.123 g, 1 mmol) were dissolved in CH (40 mL). Then MWNTs (42 mg) were added to the solution, followed by sonication for 1 h. Then, 20 mL of a solution containing 21 mg mL^{-1} of mPVCs with different degree of substitution were added, and the resulting mixture was stirred at 40 °C under nitrogen for 72 h. After cooling to room temperature, the dark suspension was centrifuged and the supernatant, containing MWNT-functionalized PVC, precipitated in methanol under vigorous stirring. The solid was filtered, washed with methanol and dried under vacuum. In order to eliminated rest of nonreacted MWNT, the solid was redissolved in THF, centrifuged at a high speed (15 000 rpm) and the supernatant solution coagulated with methanol. The procedure was repeated twice and 375.8 mg of a gray solid (yield = 89%) was obtained after vacuum-drying at 50 °C for 30 h.

Characterization. The FTIR measurements were carried out with Perkin-Elmer System 2000 FTIR spectrometer equipped with a deuterated triglycine sulfate detector (DTGS) using a resolution of 2 cm^{-1}. The samples were thoroughly mixed with KBr and pressed into pellet form. Because of the hydroscopic behavior of KBr, the sample cell was purged with desiccated air.

^{1}H NMR spectra were recorded at 400 MHz on a Varian Inova 400 spectrometer with dioxane-d_8 as the solvent and locking agent at 80 °C under standard conditions. The tacticity of parent PVC, the mPVCs, and the nanotubes covalently functionalized PVC (MWNT-mPVC) samples were measured by means of ^{13}C NMR decoupled spectra obtained at 80 °C using a Varian Unity instrument operating at 125 MHz in dioxane-d_8 solutions. The spectral width was 2500 MHz, and a pulse repetition rate of 3 s and 16 000 data points were used. The relative peak intensities of the spectra were measured from the integrated peak areas, calculated by means of an electronic integrator.

To obtain glass transition temperatures (T_g), differential scanning calorimetric scans were conducted on 8−10 mg samples with a Mettler TA4000 calorimeter. A heating rate of 10 °C/min and a calibration with indium was employed as a standard. The samples were scanned twice, and T_g was taken as the midpoint between the intersections from the glassy state to the liquid state of the second scan. The reproducibility of duplicate runs of samples with well-defined T_g's was better than ±0.2 °C.

Confocal Raman measurements were made in the Raman Microspectroscopy Laboratory of the Characterization Service in the Institute of Polymer Science & Technology, CSIC. A Renishaw InVia Reflex Raman system (Renishaw plc, Wotton-under-Edge, U.K.) employing a grating spectrometer with a Peltier-cooled charge-coupled device (CCD) detector, coupled to a confocal microscope was used. All spectra were processed using Renishaw WiRE 3.2 software. The Raman scattering was excited using a laser wavelength of 785 nm.

High resolution transmission electron microscopy (HRTEM) was carried out in a Philips Tecnai 20F FEG microscope operating at 200 kV, equipped with a scanning transmission electron microscopy (STEM) module, with a dark field high angle annular detector for *Z*-contrast imaging. For TEM measurements a few drops of samples in THF solution (with a nanotube concentration of ca. 0−1−05 mg/mL) were deposited onto the holey copper TEM grids by drop-casting and dried under vacuum.

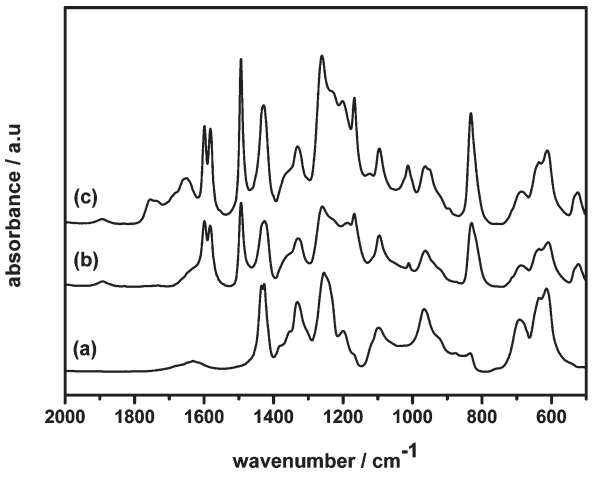

Figure 1. IR spectra of (a) PVC, (b) mPVC3, and (c) MWNT- mPVC3.

The thermal scans of the individual polymers, ozonized MWNTs and the grafting samples were performed with a Mettler TA4000/TG50 thermogravimetric analyzer (TGA) on 5−10 mg samples. The weight percentage of remaining material in the pan was recorded during heating from 30 to 900 °C at a heating rate of 10 °C/min. Nitrogen was used as the purge gas. Isothermal experiments were carried out at 160 °C for 1 h. UV−visible absorption spectra of degraded samples in HMPT solutions (of ca. 0.4 mg mL^{-1}) were measured using a Perkin-Elmer UV−vis Lambda 16 spectrometer.

The dynamic mechanical performance of the polymers was studied using a Mettler DMA 861 dynamic mechanical analyzer. Rectangular shaped samples of $\sim 19.5 \times 4 \times 0.5$ mm^3 were mounted in a large tension clamp. The measurements were performed in the tensile mode at a frequency of 1 Hz, in the temperature range between −100 and +110 °C, at heating rate of 2 °C/min. A dynamic force of 6 N was used oscillating at fixed frequency and amplitude of 30 μm.

Results and Discussion

PVC was modified by nucleophilic substitution to introduce hydroxyl pendant groups capable to form ester linkages with carboxylic groups on MWNTs. The time of the substitution reaction was varied in order to obtain samples with different degree of modification (Table 1). The incorporation of 4-hydroxythiophenolate groups into the polymer was proved by IR spectroscopy (Figure 1). In comparison to the parent polymer the mPVC display three new signals at 1497, 1587, and 1602 cm^{-1} corresponding to the aromatic C═C vibration modes, as well as an absorption band around 3400 cm^{-1} due to hydroxyl function. The success of the modification was also proved by ^{1}H NMR (Figure 2). mPVC present new signals due to aromatic (7.5−6.9 ppm) and hydroxyl protons (7.9 ppm) in comparison with pristine PVC that confirms the success of the reaction. ^{1}H NMR spectra were also employed to determine the overall composition of modified polymers. With increasing reaction time, aromatic protons as well as hydroxyl proton peaks are observed. The analysis was performed by comparing the integrated intensities of the aromatic protons signals (δ = 7.5−6.9) ppm with the signal at δ = 4.9−4.5 ppm ascribed to the methynic protons in the pure PVC units. Figure 3 shows the evolution of the degree of substitution of PVC with KHT as a function of time. As can be seen, the kinetic curve exhibits a steep period followed by a slower one in accordance with what was found with other nucleophiles[29,30]

After the esterification, the purified product, named as MWNT-mPCV*x*, were a gray powder that dissolves in organic solvents such as THF, CH, dioxane, *N*,*N*-dimethylformamide, and 1,2-dichlorobenzene, without any precipitations over time.

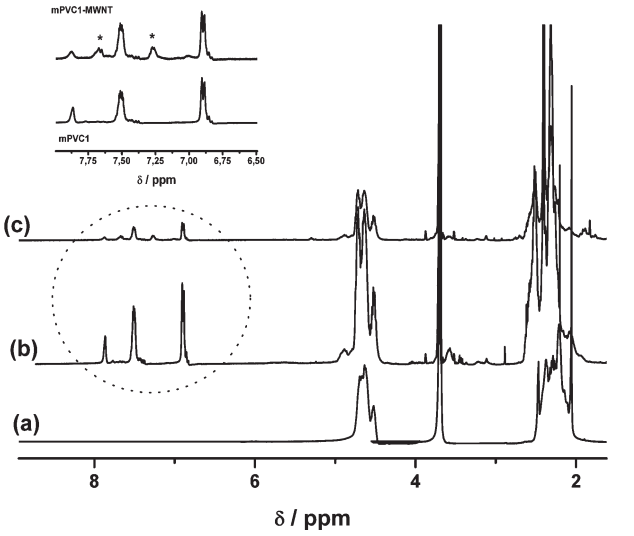

Figure 2. ^{1}H NMR spectra of (a) PVC1, (b) mPVC1, and (c) MWNT-mPVC1. The inset shows a magnified view of the aromatic protons signals for mPVC1 and MWNT-mPVC1.

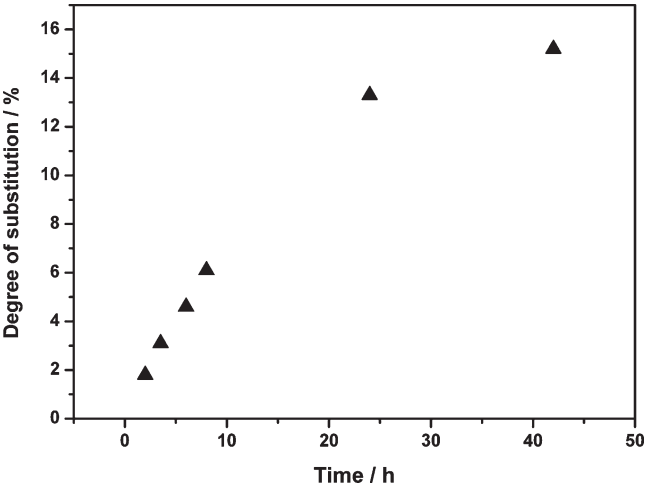

Figure 3. Kinetic curve for the nucleophilic substitution on PVC with KHT in CH at 40 °C.

At this point it is important to remark that we were interested in the study of PVC covalentely modified with MWNT. Therefore we were careful to purify the final product.The FTIR spectrum of the MWNT-mPCV1 shows absorption bands characteristic of the mPVC overlay with new bands (Figure1). The effective linkage between the MWNT and the mPVC is evident from FTIR spectrum, which shows a band at 1758 cm^{-1} corresponding to C═O stretching of ester groups. In fact, similar results have been observed in other polymer esterification reactions,[34] suggesting that esterification also took place in our system.

The solubility of the functionalized MWNT-mPVC in common organic solvents makes possible to carry out NMR characterization in solution. The ^{1}H NMR spectrum of the MWNT-mPVC1 in deuterated dioxane is quite different from that of the corresponding mPVC, especially in the zone of the aromatic and hydroxyl protons (Figure 2). First, the intensity of the hydroxyl proton peak remarkably decreases after the esterification reaction. On the other hand, two new signals at 7.21 ppm and 7.62 ppm appear. These signals correspond to aromatic protons in a different environment and can be due to the influence of the carbonyl of the ester group on the protons of the benzene ring. In fact, it is well-known that the anisotropy of the carbonyl group

Scheme 1. Simple Diagram of the Stereoselective Nucleophilic Substitution of PVC

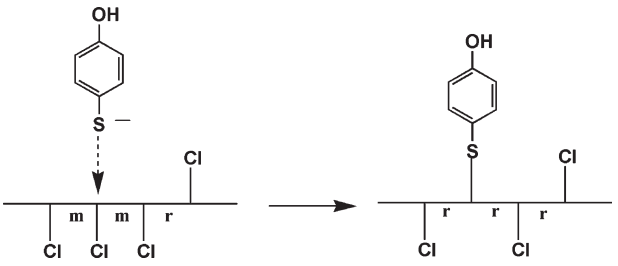

operates so as to cause deshielding giving place to downfield shifts[35] (Figure 2). This is in agreement with the fact that the degree of substitution obtained when comparing the relative integrated intensities in the range of δ = 7.5−6.9 ppm in the functionalized MWNT-mPVC1 with the methynic protons in the main chain PVC units is exactly the same that the obtained for the mPVC. Consequently, the discrimination of both types of protons, i.e. protons of the MWNT-mPVC sample and protons of the mPVC units, let us to evaluate the percentage of nanotubes in the sample. On the basis of the signals integration, the amount of carbon nanotubes in MWNT-mPVC1 was estimated to be about 1.3% units based on total composition (Figure 2). This is a reasonable value considering the low degree of substitution in the preliminary reactions that leads to a small number of active centers for esteritfication with nanotubes (Table 1). Usually, the yield of a typical esterification reaction between two simple molecules is higher that 90%. However, our system is more complex and other factors, such as steric hindrance have to be considered.

Once the covalent incorporation of MWNT to mPVC was proved, special interest has been paid to analyze some interesting aspects of the substitution reaction mechanism. The substitution reaction proceeds through a stereoselective mechanism thus leaving to a stereoselective incorporation of MWNT (a simple model is shown in scheme 1). In order to study this point, the evolution of PVC tacticity in both the modified polymer and the corresponding MWNT-mPVC, was followed by high resolution ^{13}C NMR spectroscopy. The ^{13}C NMR spectra of both mPVC and MWNT-mPVC are quite similar to that for PVC, due to their relative low degree of substitution. However, a very weak signal at ca. 140 ppm, assigned to aromatic carbon atoms, is perceived (not shown). The ^{13}C NMR spectrum of the mPVC containing 4.6% of 4-hydroxythiophenolate (mPVC1) is shown in Figure 4. In addition to signals around 57.6, 58.5, and 59.3 ppm which are due to the unreacted iso, hetero, and syndiotactic triads, respectively, it contains new peaks around 59.9−60.5 ppm, which are very close to the syndiotactic triads of unmodified PVC. We assume that these peaks at 59.9−60.5 ppm are due to modified polymer unit and originated by changes in the local microstructure after modification as has also been observed with other nucleophiles.[29] In order to check it, the evolution of the ^{13}C NMR spectrum with conversion has been analyzed (Table 1). It is clear that the isotactic triad content decreases (0.162 for mPVC1 vs 0.210 for parent PVC) while the syndiotactic triad content increases (0.337 for mPVC1 vs 0.292 for parent PVC), this being the first evidence of the stereoselectivity of the reaction (Scheme 1). As it has been previously explained,[29,30] from the integration of the content of the *mmmr* pentad (57.6−57.4 ppm), the changes in *rmmmrx* and *mmmmrx* (x = m or r) heptads, may be calculated at least to some extent. It appears evident that the overall decrease of *mmmr* content is chiefly related to the specific disappearance of the heptad *mmmmrx* (x = m or r) (Figure 4). As it can be seen, the decrease of the 57.50 ppm signal corresponding to *mmmmrx* (x = m or r) is more pronounced than that

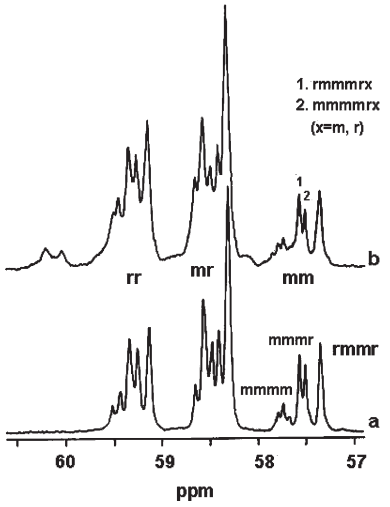

Figure 4. ^{13}C NMR spectra of (a) pristine PVC and (b) mPVC1.

at 57.56 ppm for *rmmmrx* (x = m or r). Thus, the reactivity of *mmr* proves to be much more accentuated as the length of the associated isotactic sequence increases. This agrees with previous studies using other nucleophiles.[29] Consequently, the increase of the *rmmmrx*/*mmmmrx* ratio with 4-hydroxythiophenolate incorporation (1.30 for mPVC1 vs 1.14 for parent PVC) demonstrates the stereoselective nature of the reaction.

What is especially important for the aim of the present work is to emphasize that the MWNT-mPVC retained the microstructure changes arising in the mPVC. Consequently, it can be assumed that the functionalization of MWNT is stereoselective and only takes place through the most preferential points in the polymer chain.

The FTIR results, mainly in the region of the C−Cl vibrational bands at 615 cm^{-1} and 637 cm^{-1} (Figure 1), support the stated above since it is evident that the I_{615}/I_{637} ratio increase in both modified samples as has been previously reported.[29]

It is important to note that every substitution derived from the inversion of the configuration of the carbon alters the configuration and the relative conformation of the adjacent triads, thereby generating a significant rearrangement of a specific chain segment. The above conclusion that substitution with KHT and, consequently, with MWNT proceed following a stereoselective way is further supported by results on the variation of the persistence ratio (ρ, defined by Reinmöller an Fox[36] as the ratio between the normalized intensity of isotactic diads and the conditional probability of a syndiotactic placement on an isotactic chain end), as a function of the degree of substitution for the samples (Figure S1, Supporting Information). It appears evident that ρ decreases linearly with conversion (Table 1), which means that the substitution reaction brings about a progressive deflection from Bernoullian character (around ρ = 1) toward nonbernoullian statics, similar to that found when the reaction is carried out with other nucleophiles[29,30]

In order to further verify the structure of MWNT-mPVC, Raman spectra were conducted (Figure 5). The Raman spectrum of MWNT-mPVC prepared by film evaporated from THF solutions shows the typical features of MWNT. It displays broad peaks centered at 1310 and 1600 cm^{-1} assigned to the D and G typical bands for CNTs. The analysis of the intensity ratio between the D and G band gave an I_D/I_G value of 1.67, which is much higher than that for the ozonized MWNT (I_D/I_G = 1.03) confirming its effective linkage to the mPVC. Besides the much higher Raman efficiency of the MWNT signals, weak bands of the PVC can be seen at 615−630, 699, and 1429 cm^{-1}. Furthermore, a band at 1090 corresponding to the modified polymer is

clearly observed. This band is assigned to the *S*-aryl stretching for the aromatic modifier (HT). This band is stronger in the spectrum of mPVC (Figure S2, Supporting Information). Furthermore the Raman spectrum of mPVC shows the bands of the polymer on the top of a broad fluorescent band originated in the aromatic moieties (Figure S2, Supporting Information). This fluorescent band is absent in the spectrum of MWNT-mPVC (Figure 5) and can be explained by quenching of fluorescence due to carbon nanostructures, which is an indirect evidence of the effective attachment of MWNTs.

More evidence for the presence of MWNT is collected from TEM imaging by dropping a small quantity of solution onto a holey copper grid (Figure 6). Figure 6a corresponds to the *Z*-contrast image used to localize the MWNTs and to select regions to be analyzed by high resolution TEM. From this image it is clear that the MWNT-mPVC is composed of individual nanotubes of different length ranging from hundred of nanometers to several micrometers. The nanotube marked with an arrow was further analyzed by high resolution TEM (Figure 6b). It can be observed the presence of the polymer on the walls of the nanotubes. In addition, some deformation of walls can also be seen. Therefore, as the nanotubes are insoluble and they are observed by TEM in samples deposited from THF solution, it is clear that they are covalently attached to the soluble polymer.

The incorporation of fillers into a polymer matrix can bring about changes in the mechanical and thermal characteristics of the resulting composite. Changes in intrinsic polymer properties by addition of MWNTs are indicative of nanotube-matrix interactions. For a well-dispersed system, even low nanotube volume fractions provide an enormous amount of interfacial area through which the bulk properties of the polymer can be altered. One benchmark used to compare the thermal behavior

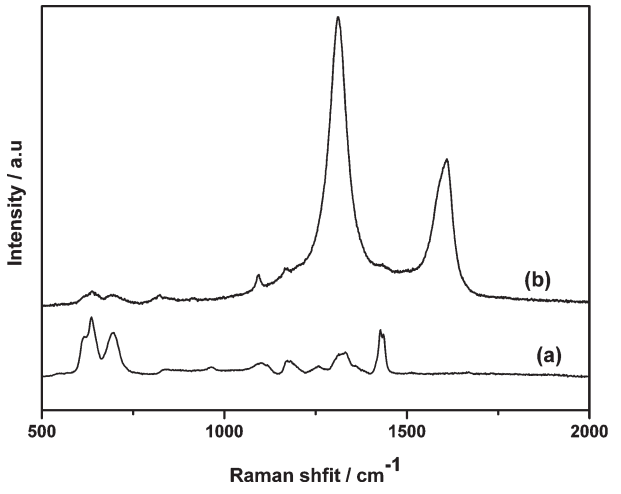

Figure 5. Raman spectra of PVC (a) and MWNTs-mPVC3 (b).

of composites is the glass transition temperature (T_g). Increases in T_g of composite systems containing MWNTs have been obtained[37] in particular in polymer-grafted nanotubes.[38,39] However, in our case it is necessary to study the evolution of T_g in the previously modified, which depends on the extension of the modification,[29] to finally compare with the MWNT-functionalized PVC. (Table 1). Changed in T_g are more pronounced at lower degree of substitution and became less marked as the modification increases. This nonlinear behavior clearly indicates that T_g depends on two well-defined factors. In fact, if the changes in T_g were the result of a simple change in the chemical composition, a steady variation should be observed. Consequently, one factor is the linking of 4-hydroxythiophenolate groups (bulkiness and possible interactions), which restricts the segmental movements, thus increasing the T_g of the polymer. The other factor is the microstructure, in terms of the isotactic and syndiotactic sequences, and especially the local configurations and conformation terminal of those sequences.[29] Thus, the T_g-determining effect of the stereospecific microstructure is unambiguously disclosed. The T_g of the MWNT-mPVC1 (92 °C) is a little higher than the obtained for mPVC1. However, for the other two samples, the values obtained in presence of grafted MWNT are similar to those in mPVC (98.7 °C for MWNT-mPVC2 and 100.6 °C for MWNT-mPVC3). The additional increase at lower substitutions is maximum approximately at the same degree of substitution as the maximum in the evolution of the rmmmrx/mmmmrx ratio with degree of substitution.[30] From this result we assume that the evolution of T_g in MWNT-mPVC1 with respect to the modified polymer is related to the respective changes in the *mmr* tetrad at the end of isotactic sequences of at least one heptad in length. In other words, the ~5 °C additional increase of T_g in MWNT-mPVC1 is a result of the local conformational rearrangements and indicates that MWNT must in some way occupy space of the large free-volume, ascribed to the $gttg^-tt$ conformation connected with sufficiently long isotactic sequences, increasing packing density. Summarizing, the T_g values for the MWNT-mPVC1 samples are particularly outstanding: exceptional shift of nearly 14 °C occurs at only 1.3% units of the MWNT. The explanation can be understood only by assuming the changes in the *mmr* tetrad especially when adopting the $gttg^-$ conformation, which is a defect-like interruption of regularity, and exhibits excess of free-volume, enhanced local rotational mobility, and restricted ability for interchain interaction. The addition of MWNT to PVC occupying space of large free-volume induces us to propose a likely local packing density and a change in the segmental motion. These results are very important to take into account in the preparation of nanocomposites between PVC and other polymers.

TGA analysis showed that the thermal stability of PVC decreased after chemical modification with KHT. In fact, the PVC decomposition occurs at 290 °C whereas for the mPVC1 it takes place at 265 °C (Figure S3, Supporting Information).

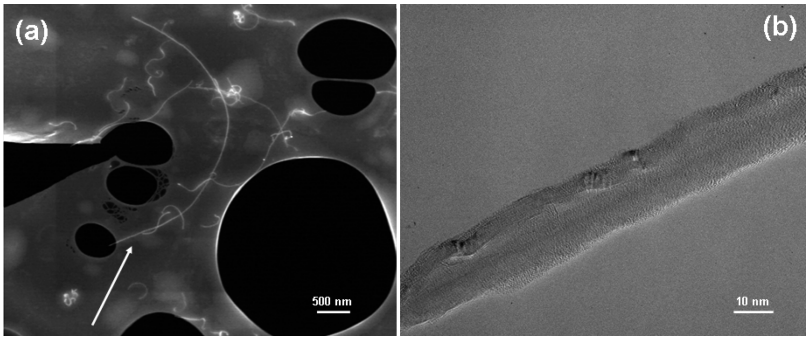

Figure 6. *Z*-Contrast dark field (a) and HRTEM (b) images of MWNT-mPVC1.

Consequently, a change of the global process of degradation is observed. This trend can be accounted for by assuming that two different processes take place in the overall degradation of PVC: one involves initiation by the unstable triad conformations $gttg^-$ (isotactic) and *tttg* (heterotactic), followed by a particular propagation. The second process involves random initiation at stable and normal structures followed by propagation to *trans* syndiotactic sequences in the chain. It was proposed that a selective substitution brings about a strong progressive stabilization until a substitution extent of ~1% is attained; afterward the stability decreases with increasing substitution. These effects were proposed to result respectively from the lability of some chloride atoms located at $gttg^-$ and *tttg* conformations, which disappear by selective substitution and from the favored building-up of all-trans polyenes upon initiation at syndiotactic sequences.[40] Actually, specific substitution at $gttg^-$ and *tttg* triads yields an increase in overall *trans* chain conformation (configuration inversion resulting from the S_N2 substitution). It is evident that dynamic TGA experiments make difficult the visual display of initial steps of thermal degradation. Nevertheless, it is interest to note that comparing the thermal degradation between the mPVC samples and the corresponding graft samples we observed an increase of ~5 °C of stability (Figure S3, Supporting Information). So, the MWNT stabilize the sample. Perhaps, the nucleophilic substitution decreases the stability, which is partly recovered after the MWNT's grafting.

Since, as indicated before, the graft reaction is stereoselective at very low grafting levels, it seemed very interesting to investigate whether the stabilization after reaction takes place so further identifying the g^+ttg^- isotactic triad conformation as being a very labile structure in PVC.[40] In case it does, supplementary evidence of the crucial role of such local conformational defects, inferred from an earlier work,[40] on the degradation and stabilization mechanisms of PVC, will be developed.

In order to elucidate this point, we had to analyze the degradation at low conversion, where the influence of chain conformations in the degradation process is more apparent. With this objective we carried out isothermal degradation at 160 °C for 1 h in nitrogen atmosphere, which represents ~1−2% loss weight. The results obtained from the isothermal degradation clearly demonstrate the higher stability of the MWNT-mPVC1. In fact, the parent PVC has a degradation rate of 1.6×10^{-2} %/min compared to 1.2×10^{-2} %/min observed for MWNT-mPVC sample, which represents a degree of stabilization of 25%. In addition, samples with higher MWNT content hardly display significant changes.

It is well established that the thermal degradation of PVC leads to the formation of polyene sequences as a result of the sequential elimination of hydrogen chloride. The characterization of these polyene sequences has been undertaken by UV/visible spectroscopy by assuming that the observed spectrum is the resultant of the overlapping spectra of a range of polyenes with different conjugated sequence lengths.[40] Consequently, the thermal stabilization of MWNT-mPVC1 should be paralleled by a strong reduction in the content of long polyene sequences compared with the parent PVC. This is in fact observed when we compare the UV−vis spectra of both samples after isothermal degradation at 160 °C (Figure 7).

The dynamic mechanical behavior of the MWNT-mPVC samples was analyzed by DMA, which provides information about the molecular relaxations that occurs in the material. The storage modulus (E') of the MWNT-mPVC samples as a function of temperature are slightly lower than of parent PVC because of the strong variation in the intermolecular interaction after previous nucleophilic substitution of PVC which hinders to visualize the expected increase of E' in those samples. The evolution of tan δ (ratio of the loss to storage modulus) as a function of

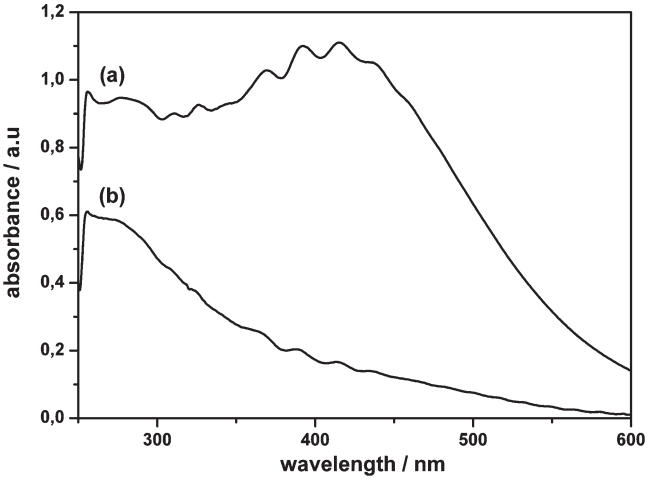

Figure 7. UV−visible spectra after isothermal treatment at 160 °C for 1 h of (a) pristine PVC and (b) MWNT-mPVC1.

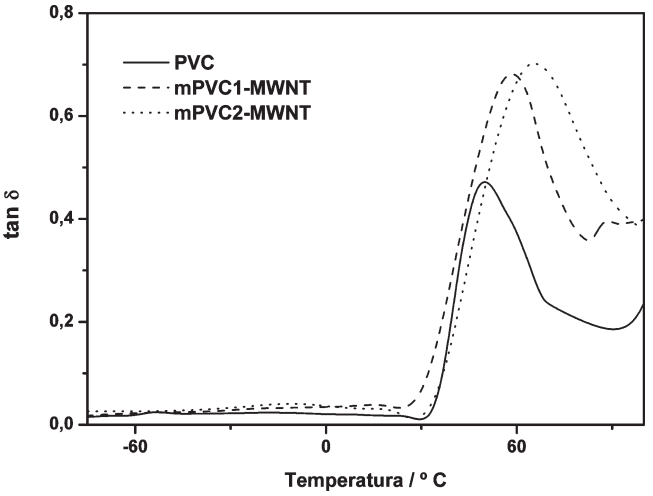

Figure 8. Variation of tan δ with the temperature of PVC and MWNTs grafted PVC.

temperature (Figure 8) reveals several relaxation peaks: the maximum at lower temperatures (β relaxation) is associated with a cooperative motion of the polymer chain and with local motions controlled by free volume fluctuations[41] and the most intense peak (α relaxation) corresponds to the T_g. By simple inspection it is evident that with increasing MWNT content, all relaxation peaks broaden and shift to the higher temperature side. This indicates that grafted fillers efficiently restrict the mobility of the PVC chains, thereby increasing the stiffness of the matrix, which is reflected in higher transition temperatures.

With respect to the α relaxation, the MWNT-mPVC samples exhibit an increase in the maximum with increasing MWNT content, which is in very good agreement with those derived from DSC thermograms. Similarly, a broadening of tan δ peak and, consequently, an increase of the area under peak with the MWNT content are observed. This was assumed as the nanotubes disturb the relaxation of the polymer chains located in their adjacent portion, pointing out the reduction in mobility imposed by the MWNT.

On the basis of the understanding above, we can see that MWNTs provide an enhancement of the microstructure effect and this opens new prospects in a huge challenge in the manufacturing of reinforced nanocomposites. The molecular level coupling between MWNT and polymer chain not only change the mobility and enhance the stability of the PVC chain but it support our opinion that molecular level couplings determine the

mechanical properties of CNT based composites. On the basis of the promising results obtained in this work, an extensive study related to the integration of the PVC-grafted MWNT in a PVC matrix for the preparation of nanocomposites is currently in progress.

Conclusions

The nucleophilic substitution of PVC with 4-hydroxythiophenolate has been shown to proceed through the local configuration-driven mechanism found in previous works for other nucleophiles. In the second instance, making use of these findings with 4-hydroxythiophenolate as the nucleophile, we have succeeded in grafting MWNT from PVC exclusively through the above quoted fraction of highly reactive isotactic triads ($gttg^-$ conformation). A higher stability of the PVC-functionalized MWNT is obtained, especially at the initial steps of thermal degradation. A considerable enhance of T_g was obtained which is a consequence of the significant rearrangement of a specific chain segment and the densification, as a function of free-volume, of the graft samples. Finally, dynamic mechanical behavior confirms that grafted fillers restrict the mobility of the polymer chains, increasing the stiffness of the matrix.

Acknowledgment. Financial support from the Spanish Ministry of Science and Innovation, MICINN (MAT2009-09335), is gratefully acknowledged. H.J.S. thanks MICINN for a Ramón y Cajal contract.

Supporting Information Available: Figures showing the variation of the persistence ratio with the degree of substitution on PVC, Raman spectrum of PVC after modification with thiophenolate, and dynamic TGA curves for PVC and its derivatives. This material is available free of charge via the Internet at http://pubs.acs.org.

References and Notes

(1) Ijima, S. *Nature* **1991**, *354*, 56–58.
(2) Baughman, R. H.; Zakhidov, A. A.; de Heer, W. A. *Science* **2002**, *297*, 787–792.
(3) Tasis, D.; Tagmatarchis, N.; Georgakilas, V.; Prato, M. *Chem.—Eur. J.* **2003**, *9*, 4000–4008.
(4) Dyke, C. A.; Tour, J. M. *J. Phys. Chem. A* **2004**, *108*, 11151–11159.
(5) Chen, J.; Hamon, M. A.; Hu, H.; Chen, Y.; Rao, A. M.; Ecklund, P. C.; Haddon, R. C. *Science* **1998**, *282*, 95–98.
(6) Hamon, M. A.; Chen, J.; Hu, H.; Chen, Y.; Ikis, M. E.; Rao, A. M.; Ecklund, P. C.; Haddon, R. C. *Adv. Mater.* **1999**, *11*, 834–840.
(7) Huang, W.; Lin, Y.; Taylor, S.; Gaillard, J.; Rao, A. M.; Sun, Y. *Nano Lett.* **2002**, *2*, 231–234.
(8) Banerjee, S.; Wong, S. S. *J. Phys. Chem. B* **2002**, *106*, 12144–12151.
(9) Banerjee, S.; Hemraj-Benny, T.; Balasubramanian, M.; Fisher, D. A.; Misewich, J. A.; Wong, S. S. *Chem. Phys. Chem.* **2004**, *5*, 1416–1422.
(10) Bahr, J. L.; Yang, J. P.; Kosynkin, D. V.; Bronikowski, M. J.; Smaley, R. E.; Tour, J. M. *J. Am. Chem. Soc.* **2001**, *123*, 6536–6542.
(11) Georgakilas, V.; Kordatos, K.; Prato, M.; Guldi, D. M.; Holzinger, M.; Hirsch, A. *J. Am. Chem. Soc.* **2002**, *124*, 760–761.
(12) Sun, Y.; Wilson, S. R.; Schuster, D. I. *J. Am. Chem. Soc.* **2001**, *123*, 5348–5349.
(13) Pekker, S.; Salvetat, J. P.; Jakab, E.; Bonard, J. M.; Forro, L. *J. Phys. Chem. B* **2001**, *105*, 7938–7943.
(14) Peng, H.; Reverdy, P.; Khabashesku, V. N.; Margrave, J. L. *Chem. Commun.* **2003**, 362–363.
(15) Ying, Y.; Saini, R. K.; Liang, F.; Sadana, A. K.; Billups, W. E. *Org. Lett.* **2003**, *5*, 1471–1473.
(16) Qin, S.; Qin, D.; Ford, W. T.; Resasco, D. E.; Herrera, J. E. *Macromolecules* **2004**, *37*, 752–757.
(17) Blake, R.; Gun′ko, Y. K.; Coleman, J.; Cadek, M.; Fonseca, A.; Nagy, J. B.; Blau, W. J. *J. Am. Chem. Soc.* **2004**, *126*, 10226–10227.
(18) Liu, Y.; Yao, Z.; Adronov, A. *Macromolecules* **2005**, *38*, 1172–1179.
(19) Tasis, D.; Papagelis, K.; Prato, M.; Kallitsis, I.; Galiotis, C. *Macromol. Rapid Commun.* **2007**, *28*, 1553–1558.
(20) Tsubokawa, N. *Polymer J.* **2005**, *9*, 637–655.
(21) Gao, C.; He, H.; Zhou, L.; Zheng, X.; Zhang, Y. *Chem. Mater.* **2009**, *21*, 360–370.
(22) Li, H. M.; Cheng, F. Y.; Duft, A. M.; Adronov, A. *J. Am. Chem. Soc.* **2005**, *127*, 14518–14524.
(23) Blake, R.; Coleman, J. N.; Byrne, M. T.; McCarthy, J. E.; Perova, T. S.; Blau, W. J.; Fonseca, A.; Nagy, J. B.; Gun′ko, Y. K. *J. Mater. Chem.* **2006**, *16*, 4206–4213.
(24) (a) Hill, D. E.; Lin, Y.; Rao, A. M.; Allard, L. F.; Sun, Y. P. *Macromolecules* **2002**, *35*, 9466–9471. (b) Sun, Y. P.; Fu, K.; Lin, Y.; Huang, W. *Acc. Chem. Res.* **2002**, *35*, 1096–1104. (c) Lin, Y.; Zhou, B.; Fernando, K. A. S.; Liu, P.; Allard, L. F.; Sun, Y. P. *Macromolecules* **2003**, *36*, 7199–7204. (d) Hill, D.; Lin, Y.; Qu, L.; Kitaygorodsky, A.; Connell, J. W.; Allard, L. F.; Sun, Y. P. *Macromolecules* **2005**, *38*, 7670–7675. (e) Gao, J.; Zhao, B.; Itkis, M. E.; Bekyarova, E.; Hu, H.; Kranak, V.; Yu, A.; Haddon, R. C. *J. Am. Chem. Soc.* **2006**, *128*, 7492–7496. (f) Bourlinos, A. B.; Georgakilas, V.; Boukos, N.; Dallas, P.; Trapalis, C.; Giannelis, E. P. *Carbon* **2007**, *45*, 1583–1595. (g) Yang, B. X.; Shi, J. H.; Pramoda, K. P.; Goh, S. H. *Compos. Sci. Technol.* **2008**, *68*, 2490–2497. (h) Zhang, W.; Sun, Y.; Wu, C.; Xing, J.; Li, J. *Anal. Chem.* **2009**, *81*, 2912–2920.
(25) Shi, J. H.; Yang, B. X.; Pramoda, K. P.; Goh, S. H. *Nanotechnology* **2007**, *18*, 375704.
(26) Suzuki, T. *Pure Appl. Chem.* **1977**, *49*, 539–567.
(27) Mukherjee, A. K.; Gupta, A. *J. Macromol. Sci. Rev. Macromol. Chem.* **1980**, *19*, 293–317.
(28) Percec, V.; Asgarzadeh, F. *J. Polym. Sci., Polym Chem.* **2001**, *39*, 1120–1135.
(29) Martínez, G.; Millán, J. *J. Polym, Sci., Polym Chem.* **2004**, *42*, 6052–6060.
(30) Martínez, G. *J. Polym, Sci., Polym. Chem.* **2006**, *44*, 2476–2486.
(31) Jung, R.; Kim, H. S.; Jin, H. J. *Macromol. Symp.* **2007**, *249−250*, 259–264.
(32) Broza, G.; Piszczek, K.; Schulte, K.; Sterzynski, T. *Compos. Sci. Technol.* **2007**, *67*, 890–894.
(33) Mamunya, Ye.P.; Levchenko, V. V.; Rybak, A.; Boiteux, G.; Lebedev, E. V.; Ulanski, J.; Seytre, G. *J. Non-Cryst. Solids* **2010**, *356*, 635–641.
(34) Yang, S. Y.; Huang, C. Y. *J. Appl. Polym. Sci.* **2008**, *109*, 2452–2459.
(35) Akitt, J. W. *NMR and Chemistry. An Introduction to the Fourier Transform-Multinuclear Era*; Chapman & Hall: New York, 1983, p 20.
(36) Reinmöller, M.; Fox, T. G. *Polym. Prepr (ACS)* **1966**, *7*, 999–1004.
(37) Cui, L.; Tarte, N. H.; Woo, S. I. *Macromolecules* **2009**, *42*, 8649–8654.
(38) Priftis, D.; Sakellariou, G.; Baskaran, D.; Mays, J. W.; Hadjichristidis, N. *Soft Mater.* **2009**, *5*, 4272–4278.
(39) Priftis, D.; Petzetakis, N.; Sakellariou, G.; Pitsikalis, M.; Baskaran, D.; Mays, J. W.; Hadjichristidis, N. *Macromolecules* **2009**, *42*, 3340–3346.
(40) Millán, J.; Martínez, G.; Gómez-Elvira, J. M.; Guarrotxena, N.; Tiemblo, P. *Polymer* **1996**, *37*, 219–230 and references cited therein.
(41) Fischer, E. W.; Hellmann, G. P.; Spiess, H. W.; Hörth, F. J.; Ecaris, U.; Wehrle, M. *Makromol. Chem. Suppl.* **1985**, *12*, 189–214.